Inverse Tone Mapping

Francesco Banterle [*]
University of Bristol

Patrick Ledda [†]
University of Bristol

Kurt Debattista [‡]
University of Bristol

Alan Chalmers [§]
University of Bristol

Abstract

In recent years many Tone Mapping Operators (TMOs) have been presented in order to display High Dynamic Range Images (HDRI) on typical display devices. TMOs compress the luminance range while trying to maintain contrast. The dual of tone mapping, inverse tone mapping, expands a Low Dynamic Range Image (LDRI) into a HDRI. HDRIs contain a broader range of physical values that can be perceived by the human visual system. The majority of today's media is stored in low dynamic range. Inverse Tone Mapping Operators (iTMOs) could thus potentially revive all of this content for use in high dynamic range display and image-based lighting. We propose an approximate solution to this problem that uses median-cut to find the areas considered of high luminance and subsequently apply a density estimation to generate an *Expand-map* in order to extend the range in the high luminance areas using an inverse Photographic Tone Reproduction operator.

CR Categories: I.3.7 [Computer Graphics]: Three-Dimensional Graphics and Realism—Color, shading, shadowing, and texture;

Keywords: Tone Mapping, Image Processing, Image Based Lighting

1 Introduction

In recent years with the increasing need and popularity of HDRIs in various fields such as physically-based renderings, movies and videogames, the issue of reproducing such vast luminance ranges on typical displays has become extremely important. This process is usually called Tone Mapping, and in the past decade many TMOs had been proposed, see [Reinhard et al. 2005] for a complete overview.

These operators can be divided into different categories depending on how they attempt to reduce contrast of an HDRI. There are models that apply the same mapping function across the image which are known as Global Operators. Examples of these include [Ward 1994; Larson et al. 1997; Tumblin et al. 1999; Drago et al. 2003]. While these algorithms are very simple, details are frequently lost in very bright and/or dark areas of the image [Ledda et al. 2005].

The other class of TMOs are known as Local Operators, in which each pixel is scaled according to the average luminance level of its local neighborhood, for example [Chiu et al. 1993; Tumblin et al. 1999]. The most difficult issue with this class of operators is the

---
[*]e-mail: banterle@cs.bris.ac.uk
[†]e-mail: ledda@.bris.ac.uk
[‡]e-mail: debattis@.bris.ac.uk
[§]e-mail:alan.chalmers@bris.ac.uk

correct determination of the size of the local neighborhood for each pixel. Indeed if it is done incorrectly, ringing artifacts, or "halos", may occur around high contrast edges. To solve this problem several approaches have been proposed, such as [Reinhard et al. 2002; Ashikhmin 2002; Fattal et al. 2002; Pattanaik and Yee 2002], that employ a series of band-pass filters or apply a multiscale decomposition into intrinsic layers, such as reflectance, illumination, texture, etc. Contrast reduction is then applied to the illumination layer.

Finally, another class of TMOs attempt to mimic the Human Visual System employing mapping functions that take account of aspects of human vision for example, [Pattanaik et al. 1998; Ledda et al. 2004].

The dual of Tone Mapping is the Inverse Tone Mapping problem. In this paper we introduce an approach for an inverse Tone Mapping Operator (iTMO). While, it has been standard practice to generate HDRI from many LDRI captured at different exposures times [Debevec and Malik 1997], the problem is considerably more difficult when using a single LDRI. Clearly the problem is unconstrained as we do not have the ratio image [Ward and Simmons 2005] for tonemapped HDRIs, and we do not know any information from standard 8bit images except the given exposure.

Since HDR capturing was introduced only in the last decade [Debevec and Malik 1997], Inverse Tone Mapping could make available in HDR the media of 180 years of photography and more 100 years of cinematography. All of this material was taken not in HDR, and it can represent places, people and historical events that do not longer exist. iTMOs could enhance this material for new display devices. Also none of this material can be used to light synthetic scenes in Image Based Lighting applications, as using LDRI in Image Based Lighting can only achieve soft shadows.

Furthermore, in fields such as Visual Effects, Image-based lighting is becoming more popular therefore the need for panoramic HDR images are fundamental. Unfortunately, it is still quite rare that such images are captured due to the extremely limited time constrains on movie sets. Taking multiple photographs, is often too time consuming and therefore expensive. The importance of inverse tone mapping becomes clear since only one photograph needs to be taken.

Image Based Lighting is very important field in Computer Graphics, because it is very useful to improve the realism and to insert an object in real scene [Debevec 1998]. Indeed it plays a key role in modern Visual Effects productions however as mentioned above, due to time constraints often only a single exposure image can be captured. Although a few studios have HDR panoramic cameras these are very expensive and still slow to capture the entire range [SpheronVR ; PanoScan].

Finally, we are not aware of commercialy available off the shelf HDR videocameras, so there is no video content available for HDR display [Seetzen et al. 2004], except synthetic videos or HDR steady camera techniques, which suffer from flickering in animation. An experimental technique presented in [Kang et al. 2003] can acquire HDR videos but it is quite limited; the frame rate is low and can not acquire rapid motion, very large brightness ranges, and it sometimes produces artifacts. In this case an iTMO could be useful to enhance existing content and use this for simulations, games, and visualization of photographs.

1.1 Related Work

Our work can be related to a number of techniques that have been developed and can be found in various tutorials on graphics web sites that present techniques to expand the range in LDRI [Landis 2002]. These techniques can be classified as a simple linear or exponential expansion of the values of pixels that reach a certain threshold k to a maximum value. The main problem of this approach is that there is no space knowledge of the neighbor pixels, and this implies no knowledge of where light sources are. This can lead to noise problems, and bright pixels around low brightness areas, Figure 1. Another serious issue is that there can be areas that change very sharply and in an unnatural way, we call these areas block area, Figure 1.

In [Bennett and McMillan 2005] a video processing technique is presented in which HDR concepts are used to improve the quality of videos for removing noise and tonemapping underexposed video. However they did not look into the problem of creating a HDR video from a LDR video.

Finally our work can be related in aim to existing image editing unconstrained techniques [Khan et al. 2006] in which the user can change the material properties of a selected object in an image. Or colorization algorithms that try to colorize gray scale images, for example [Levin et al. 2004].
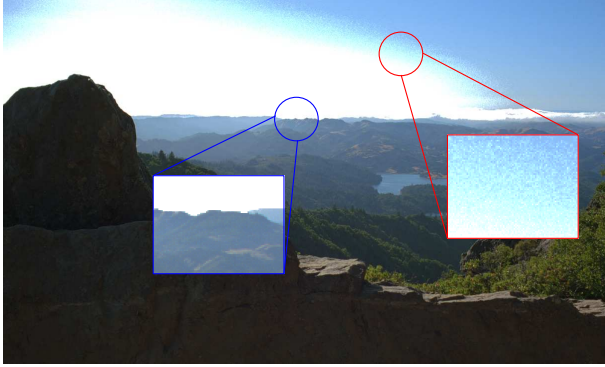

Figure 1: An example of naive techniques to expand the range: the red circle show the noise problem. The blue circle shows the block area problem.

2 Outline

The algorithm performs the following steps, Figure 2:

1. An initial HDRI is generated by applying the Inverse Tone Mapping Operator;

2. Median Cut Algorithm [Debevec 2005] is applied for finding the areas of high luminance;

3. An *Expand Map* is created from density estimation of the areas of high luminance found using Median Cut result;

4. The final HDRI is composed through linear interpolation of LDRI with the initial HDRI generated at the first step using the *Expand Map* as interpolation weights.
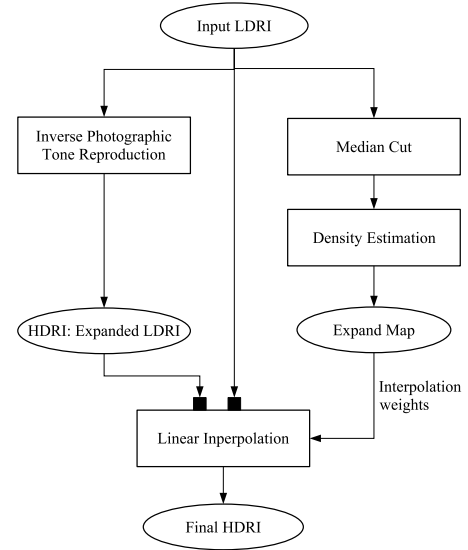

Figure 2: An overview of the proposed algorithm: firstly we create an Expanded LDRI using an inverse Photographic Tone Reproduction. Secondly we generate the *Expand Map* which is the result of density estimation of light sources created by Median Cut on LDRI. Finally the Original LDRI and Expanded LDRI are linearly interpolated using the *Expand Map*.

2.1 Inverse Tone Mapping Operator

Recently published TMOs usually take the world luminance L_w values and produce a set of luminance values L_d [Reinhard et al. 2005]. Where L_w is defined as:

$$L_w = 0.213R_w + 0.715G_w + 0.072B_w \qquad (1)$$

where R_w, G_w, and B_w respectively are red, green and blue world color. To compress the values the following equation is applied:

$$\begin{bmatrix} R_d \\ G_d \\ B_d \end{bmatrix} = \begin{bmatrix} L_d \frac{R_w}{L_w} \\ L_d \frac{G_w}{L_w} \\ L_d \frac{B_w}{L_w} \end{bmatrix} \qquad (2)$$

where R_d, G_d, and B_d are respectively red, green and blue compressed colors. For solving the inverse equation we have:

$$\begin{bmatrix} R_w \\ G_w \\ B_w \end{bmatrix} = \begin{bmatrix} L_w \frac{R_d}{L_d} \\ L_w \frac{G_d}{L_d} \\ L_w \frac{B_d}{L_d} \end{bmatrix} \qquad (3)$$

However, when starting from a LDRI we do not have any notion about $L_w(x,y)$, but only on R_d, G_d, and B_d.

The expansion of the range in a LDRI could be done in many ways; artists from visual effects productions usually apply to pixel a scaling or an exponential function [Landis 2002]. This technique can work in some cases, but in general it does not create convincing results, so we decided to solve the problem of expanding the range in a more accurate way. An alternative approach, which we adopt, is to reverse a TMO. As metioned above it is a unconstrained problem, but convincing results can be achieved by making some assumptions.

Our first step is to choose a TMO; several exist, each with their own advantages and disadvantages. For our iTMO we chose to

reverse the Photographic Tone Reproduction in its is global version [Reinhard et al. 2002]. The main reason for choosing this TMO is that it is quite easy to reverse, and also it is popular for Tone Mapping, since it performed better than other TMOs in terms of contrast loss during range compression [Smith et al. 2006], and in a series of psychophysics experiments [Ledda et al. 2005] when evaluating TMOs against an HDR display reference.

Before describing the details of our inversion method we briefly present the global version of Photographic Tone Reproduction. Initially the TMO scales pixels of the image using geometric average $\overline{L}_{\text{w}}$, this is an approximation of the key of the scene, which indicates if a scene is subjectively light, normal, or dark. This scaling is given by the following equation:

$$L_{\text{m}}(x,y) = \frac{\alpha}{\overline{L}_{\text{w}}} L_{\text{w}}(x,y) \tag{4}$$

where α is a user parameter that can be estimated from the image [Reinhard 2002], and $\overline{L}_{\text{w}}$, the geometric average, is defined as:

$$\overline{L}_{\text{w}} = \exp\left(\frac{1}{N} \sum_{x,y} \log\left(\delta + L_{\text{w}}(x,y)\right)\right) \tag{5}$$

where δ is a small non negative value, and N is the number of pixels in the image. Finally the values are compressed by the following function:

$$L_{\text{d}}(x,y) = \frac{L_{\text{m}}(x,y)}{1 + L_{\text{m}}(x,y)} \tag{6}$$

The chief problem with this function is that the highest luminance value in the image will never be mapped to 1. Also it might be desirable to burn out high luminance pixel for artistic purposes. This problem is solved by blending Equation 6 with a linear mapping:

$$L_{\text{d}}(x,y) = \frac{L_{\text{m}}(x,y)\left(1 + \frac{L_{\text{m}}(x,y)}{L_{\text{white}}^2}\right)}{1 + L_{\text{m}}(x,y)} \tag{7}$$

where L_{white} denotes the smallest luminance value that will be mapped to white.
To inverse the TMO, we need to solve in L_{m} from Equation 6 or Equation 7. The result of inversion of the first Equation is the following:

$$L_{\text{m}}(x,y) = \frac{L_{\text{d}}(x,y)}{1 - L_{\text{d}}(x,y)} \tag{8}$$

then substituting Equation 4 in the previous equation we obtain:

$$L_{\text{w}}(x,y) = \frac{L_{\text{d}}(x,y)\overline{L}_{\text{w}}}{\left(1 - L_{\text{d}}(x,y)\right)\alpha} \tag{9}$$

There are two problems for the above equation. Firstly the 1 luminance value is mapped to infinity which is not desirable. To account for this, we need a damping factor. Secondly it is not possible to control well the range to expand. In fact, very high luminance values are mapped on the highest maximum value chosen by user (the maximum value is driven using α and the damping factor), while middle and low luminance values are mapped on very low luminance values, Figure 3. Instead of the above approach, we opted to solve for L_{m} re-arranging Equation 7:

$$\frac{L_{\text{m}}^2(x,y)}{L_{\text{white}}^2} + L_{\text{m}}(x,y)\left(1 - L_{\text{d}}(x,y)\right) - L_{\text{d}}(x,y) = 0 \tag{10}$$

then substuting Equation 4 we obtain:

$$\frac{\alpha^2}{L_{\text{white}}^2 \overline{L}_{\text{w}}^2} L_{\text{w}}^2(x,y) +$$
$$+ \frac{\alpha}{\overline{L}_{\text{w}}}\left(1 - L_{\text{d}}(x,y)\right)L_{\text{w}}(x,y) - L_{\text{d}}(x,y) = 0 \tag{11}$$

Image Name	HDRI	LDRI	TONEMAPPED
Alhambra3	0.019511	0.018965	0.284269
AtriumMorning	0.284378	0.202698	0.243726
AtriumNight	0.076215	0.075131	0.272415
BristolBridge	0.028821	0.028131	0.224723
ChurchWindow1	0.002905	0.002697	0.239985
Clockbui	0.002826	0.002636	0.280020
Colorcube	0.001540	0.001388	0.250926
Couple	0.008118	0.007776	0.255610
Dani_Belgium	0.001598	0.001598	0.267191
Dani_Cathedral	0.049861	0.043159	0.239216
Dani_Synagogue	0.321129	0.302462	0.281919
Desk_oBA2	0.119672	0.079009	0.187675
Eucalyptus_Grove	1.205781	0.447119	0.34845
Galileo_tomb	0.378422	0.356415	0.309129
Grace_Cathedral	0.040209	0.036034	0.254408
Hercules_Cave1	0.013785	0.013037	0.230455
Hotel	0.373111	0.307517	0.282104
ItalianChurch1	0.008473	0.008196	0.298908
ItalianMuseum1	0.006467	0.006156	0.289998
Temple	0.078451	0.067611	0.216348
Lamp	0.165595	0.163474	0.307505
Memorial	0.031256	0.029504	0.276244
MtTamWest_o281	0.132048	0.100824	0.206138
Nave_o366	0.172494	0.147410	0.287591
Napa_Valley	0.048545	0.047631	0.262453
Still_Life	0.001916	0.001734	0.192833
St_Peters	0.350107	0.336801	0.317300
Tahoe1	0.039601	0.039030	0.280015
Tree_oAC1	0.073774	0.056163	0.198197
Uffizi	0.274167	0.190992	0.249118
Wreathbu	0.003593	0.003372	0.251488

Table 1: The values of geometric average for various HDRIs. The column labelled HDRI represents the values for original HDRI, the column LDRI represent the values for a single exposure image extracted from HDRI (the same for all images). Finally in the column TONEMAPPED are the values for the tonemapped HDRI using the global version of Photographics Tone Reproduction. The mean of absolute error between HDRI and LDRI is $\mu = 0.091766$ and the variance is $\sigma^2 = 0.006694081$. The mean of absolute error between HDRI and Tonemapped is $\mu = 0.255$ and the variance is $\sigma^2 = 0.182601$.
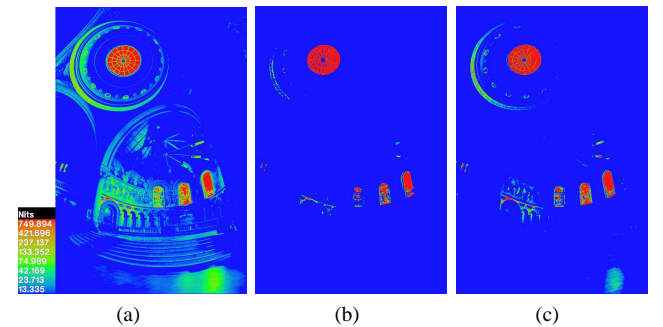

Figure 3: Comparison in false color HDRIs using logarithm 2 scale: a) Original Memorial HDR. b) Inverse Tone Mapped Memorial using Equation 9 image with 20 as a maximum luminance value. c) Inverse Tone Mapped Memorial using Equation 9 image with 200 as maximum luminance value. In b) and c) middle and low tones are mapped to very low luminance value.

This new formulation is a second order equation in $L_w(x,y)$ that can be solved easily using the quadratic formula. However, we want to solve it starting from a LDRI so there are a number of unknowns: the scaling factor α, the white point L_{white}, the geometric average $\overline{L}_w$ and the tone mapped luminance L_d.

We can approximate the original geometric average $\overline{L}_w$ using the geometric average of the LDRIs. This approximation will not work very well for overexposed or unexposed LDRI, because the value will be much higher or lower than the associated hypothetical HDRI. However, we are working with LDRIs in which $\overline{L}_w$ does not change too much with respect to the associated value for the HDRI. In fact, we noticed that this value is nearly the same for the most common test HDRIs, which include a very broad number of lighting conditions, see Table 1. Although this is not true for tonemapped HDRI (in this case we observed values between 0.2 and 0.3), we obtained good results using it for this kind of LDRIs.

The parameter $L_d(x,y)$ in Equation 11 is equal to $L'_w(x,y)$ the luminance of the tone mapped version. This can be simply observed from Equation 2. So we use it for all LDRIs. Obviously, this value is approximated for a single exposure image, but it works fine under the hypothesis mentioned before, that is not too over or under-exposed images.

The last two parameters left are α and L_{white}. They can not be derived from image. The parameter α is quite cryptic. So for an easy understanding we introduced the value L'_{max} which is the maximum luminance value expected for the inverse tone mapped image, and it is chosen by user. If we consider that the maximum luminance value in a LDRI is 1, we can derive from the quadratic solution of Equation 11 the following relation:

$$L'_{max} = \frac{L_{white}\overline{L}_w}{\alpha} \qquad (12)$$

which leads for α:

$$\alpha = \frac{L_{white}\overline{L}_w}{L'_{max}} \qquad (13)$$

Also L_{white} is set by user. We noticed that this parameter drives the expansion for the original middle and low luminance values. If L_{white} is very high those values are mapped to very low luminance values. On the other hand, if L_{white} is very low, the inverse tone mapped image will have luminance values near to the original LDRI scaled by L'_{max}. We found that good values for L_{white} that keep middle and low luminance values as the original LDRI are values with the same order of L'_{max}, Figure 4.

Finally, we can solve Equation 11. This equation always has two solutions. In fact $L_d(x,y)$ is always a non-negative value so the determinant of quadratic equation is always positive:

$$\left(\frac{\alpha}{\overline{L}_w}\left(1-L_d(x,y)\right)\right)^2 + 4\frac{\alpha^2}{L^2_{white}\overline{L}^2_w}L_d(x,y) \geq 0 \qquad (14)$$

We chose the positive solution with highest value, because it is equal to the real value of $L_w(x,y)$ if we commenced with the real values of all parameters.

The main advantage of this iTMO is that the function is smooth so it avoids noise of the naive algorithm (due to threshold). On the other hand the main problem is that we cannot expand the range arbitrarily. It works only when expanding to a medium dynamic range. Otherwise, if the value of the highest luminance is set to very high we obtain blocky effects. An efficient way to solve this problem is to create an interpolation map that interpolates pixels which belong to the high luminance areas. This map, which we
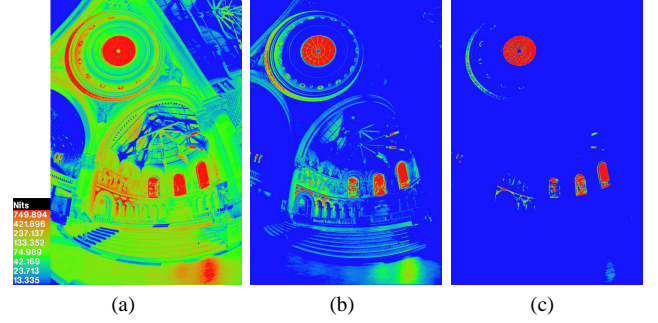

Figure 4: Comparison in false color of Inverse Tone Mapped Memorial HDRIs with 20 as maximum luminance using logarithm 2 scale: a) HDRI using $L_{white} = 1$, in this case too many pixels are expanded as can happen in a linear scale. b) HDRI using $L_{white} = 10$ in this case the values of original middle and low luminance value are nearly kept as before, and original high luminance values are expanded smoothly. c) HDRI using $L_{white} = 100$ in this case the values of original middle and low luminance value are mapped to very low luminance value, while original high luminance value near 1 are mapped on the maximum luminance chosen by user.

Image Name	Our Algorithm		Naive Algorithm	
	$P(X) \geq 0.75$	$P(X) \geq 0.95$	$P(X) \geq 0.75$	$P(X) \geq 0.95$
Alhambra3	0.09	0.02	0.49	0.32
AtriumMorning	25.18	22.24	34.01	29.26
AtriumNight	5.90	4.75	16.83	12.70
BristolBridge	10.72	7.78	20.95	14.69
ChurchWindow1	12.17	8.88	16.82	12.48
Clockbui	18.76	12.79	36.27	27.44
ColorCube	14.25	10.34	22.49	16.88
Couple	1.62	0.93	2.27	1.43
Dani_Belgium	19.02	16.19	40.73	33.48
Dani_Cathedral	7.12	4.54	10.38	6.79
Dani_Synagogue	9.40	5.33	28.16	17.75
Desk_oBA2	15.96	11.30	27.39	19.34
Eucalyptus_Grove	15.96	11.37	24.41	22.79
Galileo_Tomb	38.17	32.59	47.83	41.64
Grace_Cathedral	6.26	4.27	16.71	13.18
Hercules_Cave1	8.05	5.82	23.70	17.49
Hotel	16.79	12.69	21.68	17.55
ItalianChurch1	3.88	2.49	6.01	3.5 7
Italian_Museum	0.04	0.01	0.43	0.22
Lamp	8.61	6.45	9.60	7.89
Memorial	2.65	1.97	4.75	3.43
MtTamWest_o281	7.04	5.06	8.05	5.82
Nave_o366	8.97	7.46	14.87	11.85
Napa_Valley	4.14	3.34	6.65	5.11
Still_Life	2.34	1.75	3.84	2.74
St_Peters	22.86	18.07	38.0	31.48
Tahoe1	10.54	7.80	13.97	10.91
Temple	5.12	2.89	9.13	4.76
Tree_oAC1	7.02	4.46	8.62	6.30
Uffizi	3.53	2.42	5.28	3.24
Wreathbu	10.43	7.31	23.41	16.84

Table 2: VDP HDR results: we compared the original HDRIs with HDRIs created using our algorithm. Also we compared the original HDRIs with HDRIs generated using the naive algorithm, that expands pixels that satisfy a threshold. In both algorithms used we started from a single exposure of the original HDRI (stop 0). The columns $P(X) \geq 0.75$ and $P(X) \geq 0.95$ with $X =$ detection mean that the probability to detect the difference is more than 0.75 and 0.95 for a certain percentage of pixels. The algorithm presented performs better than *naive* algorithm with a lower percentage of pixels detected by VDP metric.

call *Expand Map*, is generated from the result of density estimation of the high luminance areas present in the image found using the Median Cut algorithm.

2.2 Finding Light Sources

The Median Cut algorithm can be used for sampling light sources for IBL [Debevec 2005]. The advantages of this algorithm is that it clusters light sources near areas of high luminance.
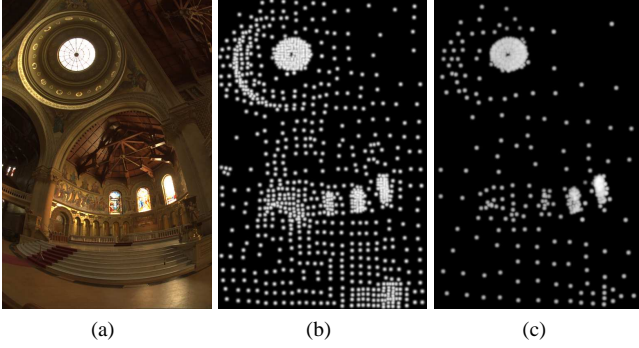

(a)   (b)   (c)

Figure 5: Comparison of median cut results using an HDRI and LDRI of Memorial HDRI: a) The memorial LDRI. b) Median cut result, 1024 light sources generated starting from a LDRI c) Median cut result, 1024 light sources generated starting from a HDRI.

The algorithm splits images into 2^n regions of similar light energy. The splitting axis is chosen as the longest dimension such that its luminance is divided evenly. Finally, it places a light source in the centroid of each region and sets the light source color to the sum of pixels values within the region. In our implementation we store the area of high luminance (equivalent to the lights in the traditional version) found in a 2D-Tree to speed-up the nearest neighbors search during the calculation of the *Expand Map*. Additionally, we do not scale the pixels for the cosine for normal images as proposed in [Debevec 2005], since we do not need to compensate the area distortion present in logitudine-latitudine images. Applying Median Cut to a LDRI and to the equivalent HDRI can produce different results. However the lights sources distribution on the LDRI maintains some features of the distribution using HDRI, Figure 5.

2.3 The Expand Map

The *Expand Map* is a map with the list of pixels to be expanded. We do not use a binary map to avoid a blocky transition between areas. A better solution will be a map in which, for each pixel, there is a weight associated. In other words, we want to identify a list of pixels that when expanded would achieve smoothly transitions between pixels. One solution to the problem is density estimation (see [Duda et al. 2001] for more details), a statistical technique that constructs an estimate, based on observed data (in our case the areas of high luminance). This technique has already been successfully used in the field of computer graphics, for example in Photon Mapping [Jensen 2001].

The idea behind the use of density estimation is to determine for each pixel x the density of high luminance areas inside an area of influence which is a circle defined by the radius r_t. The basic formula for density estimation is:

$$\Lambda(x, r_t) = \frac{\sum_{p \in \mathscr{P}} \Psi_p}{\pi r_{max}^2} \qquad (15)$$

where $\Lambda(x)$ is the estimate at point $x(i, j)$ in the image, Ψ_p is the luminance value for the point of high luminance p, $\mathscr{P}$ is the set of all high luminance points inside the area of influence given by radius r_t from $x(i, j)$, and r_{max} is the distance of the farthest light source $\Psi_{max} \in \mathscr{P}$ inside the area of influence.

The estimate can be improved using a smoothing filter. In our work, we used a Gaussian filter which is defined by the weight of the kernel given by:

$$w_p^g = \gamma \left[1 - \frac{1 - e^{-\beta \frac{d_p^2}{2r_{max}^2}}}{1 - e^{-\beta}} \right] \qquad (16)$$

where γ and β are parameters of the filter, we usually set $\gamma = 0.918$ and $\beta = 1.953$ (see [Pavicic 1990] for details). This filter is normalized so we have only to scale the luminance by w_p^g:

$$\Lambda(x, r_t) = \sum_{p \in \mathscr{P}} \Psi_p w_p^g \qquad (17)$$

In our tests we used a radius r_t of 16 pixels. An important issue is to insert a threshold for the number of light sources inside A_x otherwise the density map is very broad and false light regions can be recovered. We found that a threshold of 4-6 light sources is enough for 1024 generated light sources, Figure 6.

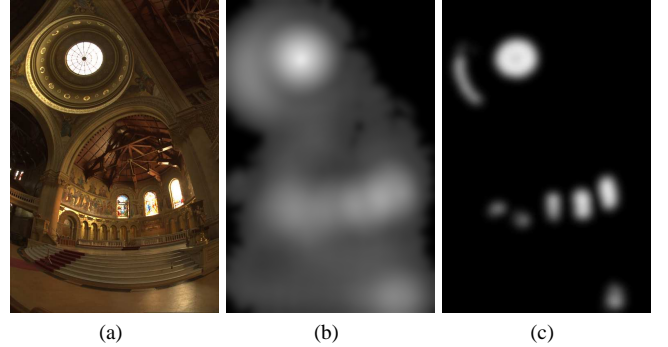(a)   (b)   (c)

Figure 6: An example of Density Estimation using Gaussian Filter: a) the memorial LDRI b) the density map calculated using a radius of 16 pixels and a threshold of one light sources, in this case we can not recover the density map properly. c) the density map calculated using a radius of 16 pixels and a threshold of 4 light sources, in this case we can recover the correct density map around the light sources.

The final stage of the algorithm is to combine the original LDRI and the expanded LDRI using the *Expand Map*, which has values in the range $[0, 1]$. Therefore these values can be used as weights for a linear interpolation between the two images.

3 Results

The main applications of our work are Image Based Lighting and in general photographs and videos sequences enhancement.

We validated our iTMO using the Visible Differences Predictor (VDP) metric proposed in [Daly 1993], in particular we used the HDR version presented in [Mantiuk et al. 2004; Mantiuk et al. 2005] and free downloadable [VDP-HDR]. This metric is based on what the Human Visual System can perceive as differences for a pair of HDRIs, which is more perceptually accurate than other metrics such as the Signal to Noise Ratio (SNR). The VDP-HDR creates a new image, called a probability map of detection, which

assigns the probability that the difference can be noticed for each pixel. For an easy understanding of the map created, we decided to use the percentage of pixels in an image when probability of detection $P(X)$ exceeds 0.75 and 0.95.
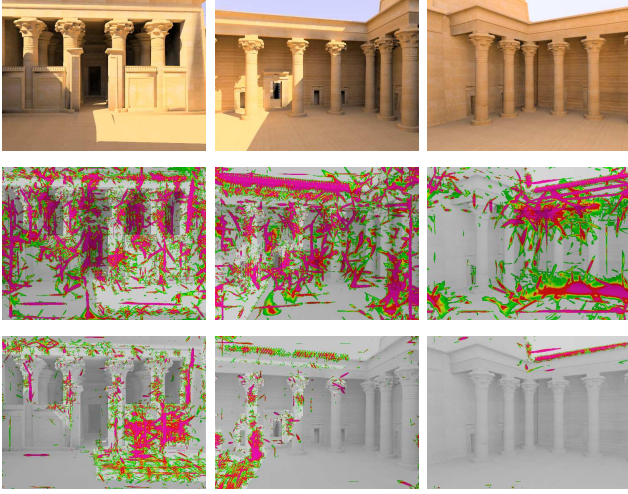

Figure 7: An example of an enhancement of LDR video. The used video represents a daylight animation around the Kalabsha temple, we generated a LDR video at the exposure stop -2. The first row shows the tonemapped frames of the video, and in the second row the VDP results of comparison of these frames between the original HDR video and the one generated using the *naive* technique. Finally, in the third row VDP results of the three frames between HDR video and the one generated using the presented algorithm are shown.

We tested the quality of our algorithm for the enhancement of photographs. For our test we generated HDRIs using our algorithm starting from a single exposure of a HDRI (stop 0), because it is the same condition of taking a picture. Starting from a tonemapped image it is hard to understand if the iTMO works well thanks to non linear transformation applied by a TMO. Then we compared these generated HDRIs with the original HDRI using VDP HDR. Also we compared the original HDRIs with HDRIs generated using the *naive* algorithm [Landis 2002] in which pixels over a certain threshold are expanded exponentially. From the results in Table 2, we show that algorithm presented in this paper perfoms better than the *naive* algorithm, on average it performs 50% better. Also the percentage of pixels detected is quite low with an average of 10.32% for $P(X) \geq 0.75$ and 8 for $P(X) \geq 0.95$.

We also tested our algorithm for Image Based Lighting application. In this case a simple scene was modelled with a plane and the Lucy model, illuminated using lightprobes, Figure 8. This scene was rendered using a standard Monte Carlo Raytracer with Importance Sampling strategy for environment maps sampling (see [Pharr and Humphreys 2004] for details). In this case we applied VDP HDR to the generated images, and our algorithm again performed better than the *naive* algorithm.

The last test considered the enhancement of LDR video. We used a HDR video sequence representing the Kalabsha temple in daylight. From the original HDR sequence, a LDR video was created by taking a single exposure (stop -2 because it is a very bright scene). Then the iTMO with standard settings was applied without the *Expand Map*, because using the standard settings (for radius r_t and number of lights threshold) for each frame, flickering can occur. We compared the video using the *naive* algorithm using VDP HDR, Figure 7. In this case the averages of the percentage of pixels in which differences are detected with a probability of more than 0.75 and 0.95 are respectively $\mu_{0.75} = 5.9$ and $\mu_{0.95} = 3.4$
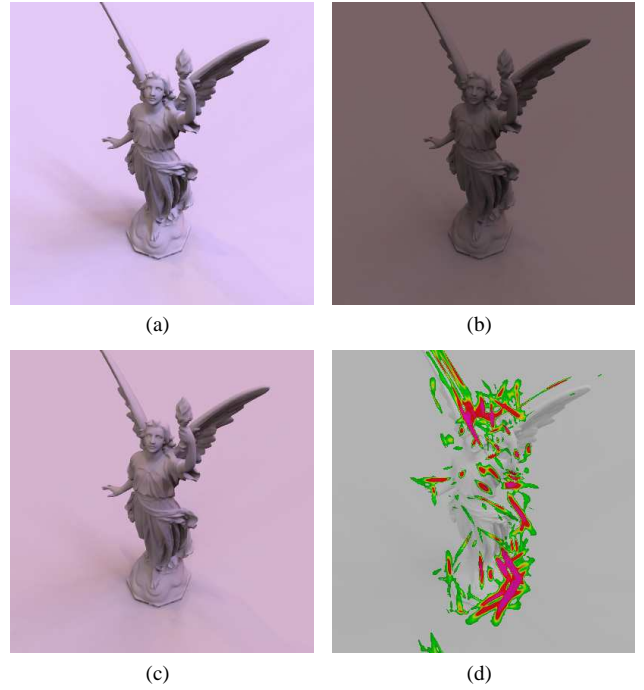

Figure 8: An example of Image Based Lighting: a) Lucy rendered using original HDRI Grace Cathedral. b) Lucy rendered using a LDRI Grace Cathedral (stop=0). c) Lucy rendered using computed HDRI Grace Cathedral computed using our algorithm. d) The VDP HDR comparison between a) and c) with a percentage of 3.07% for $P(X) \geq 0.75$, and 1.34% for $P(X) \geq 0.95$.

with the following variances $\sigma_{0.75}^2 = 17.7$ and $\sigma_{0.95}^2 = 17.9$ for our algorithm. For the *naive* algorithm the averages are $\mu_{0.75} = 25.8$ and $\mu_{0.95} = 17.7$ with the following variances $\sigma_{0.75}^2 = 34.5$ and $\sigma_{0.95}^2 = 23.0$. The test shows that our algorithm can better enhance video than *naive* one, avoiding flickering caused by blocky areas and noise. In this case we achieved good results without the *Expand Map* because the images of sequence are overall bright, and there are no localized light sources such as windows or lamps.

4 Conclusion and Future Work

We presented a new operator for LDRIs, the Inverse Tone Mapping Operator. As the results show this iTMO performs well for IBL, photographs and video sequences dynamic range enhancements in general. It is based on the inversion of Global Photographic Tone Reproduction operator and an *Expand Map* built using density estimation of light source generated by Median Cut.

We achieved better image quality than with the *naive* algorithm, and we removed noise and blocky effects that can be seen in this algorithm.

The iTMO problem is unconstrained, so we made some hypothesises about the image. The main hypothesis is an input image (or a sequence of images in case of videos) with a well balanced number of dark, normal and bright regions. If this is not the case the iTMO and *Expand Map* can not create convincing results.

The main problem of our algorithm is video processing. In that case we can not use the *Expand Map*, because it can vary enough at each frame to create flickering in the video. Also to calculate the best possible *Expand Map* user interaction is sometimes needed

to set the parameters of the density estimation (radius, number of light sources at least). Therefore we can enhance videos only using iTMO, in order to have smooth results. And this is a very big limit to the range that we want to expand, as we have shown before.

In future, we would like to explore other TMOs to reverse, or to design ad hoc iTMO in order to improve the quality. Also we will develop some heuristics for estimating the parameters of density estimation to generate *Expand Map*, which is very important task for video sequences. We know that will not eliminate all flickering problems, so we intend to generate *Expand Map* every 4-5 frames and to interpolate the in between frames using an approach similar to [Agarwala et al. 2004] to track the maps.

5   Acknoweldgement

References

AGARWALA, A., HERTZMANN, A., SALESIN, D. H., AND SEITZ, S. M. 2004. Keyframe-based tracking for rotoscoping and animation. *ACM Trans. Graph. 23*, 3, 584–591.

ASHIKHMIN, M. 2002. A tone mapping algorithm for high contrast images. In *EGRW '02: Proceedings of the 13th Eurographics workshop on Rendering*, Eurographics Association, Aire-la-Ville, Switzerland, Switzerland, 145–156.

BENNETT, E. P., AND MCMILLAN, L. 2005. Video enhancement using per-pixel virtual exposures. *ACM Trans. Graph. 24*, 3, 845–852.

CHIU, K., HERF, M., SHIRLEY, P., SWAMY, S., WANG, C., AND ZIMMERMAN, K. 1993. Spatially Nonuniform Scaling Functions for High Contrast Images. In *Proceedings of Graphics Interface '93*, Morgan Kaufmann, San Francisco, CA, 245–253.

DALY, S. 1993. *The visible differences predictor: an algorithm for the assessment of image fidelity*. MIT Press, Cambridge, MA, USA.

DEBEVEC, P. E., AND MALIK, J. 1997. Recovering high dynamic range radiance maps from photographs. In *SIGGRAPH '97: Proceedings of the 24th annual conference on Computer graphics and interactive techniques*, ACM Press/Addison-Wesley Publishing Co., New York, NY, USA, 369–378.

DEBEVEC, P. 1998. Rendering synthetic objects into real scenes: bridging traditional and image-based graphics with global illumination and high dynamic range photography. In *SIGGRAPH '98: Proceedings of the 25th annual conference on Computer graphics and interactive techniques*, ACM Press, New York, NY, USA, 189–198.

DEBEVEC, P. 2005. A median cut algorithm for light probe sampling. In *ACM Siggraph 2005 Posters*.

DRAGO, F., MYSZKOWSKI, K., ANNEN, T., AND CHIBA, N., 2003. Adaptive logarithmic mapping for displaying high contrast scenes.

DUDA, R. O., HART, P. E., AND STORK, D. G. 2001. *Pattern Classification 2nd Edition*. Wiley Interscience.

DURAND, F., AND DORSEY, J. 2000. Interactive tone mapping. In *Proceedings of the Eurographics Workshop on Rendering Techniques 2000*, Springer-Verlag, London, UK, 219–230.

FATTAL, R., LISCHINSKI, D., AND WERMAN, M. 2002. Gradient domain high dynamic range compression. In *SIGGRAPH '02: Proceedings of the 29th annual conference on Computer graphics and interactive techniques*, ACM Press, New York, NY, USA, 249–256.

JENSEN, H. W. 2001. *Realistic image synthesis using photon mapping*. A. K. Peters, Ltd., Natick, MA, USA.

KANG, S. B., UYTTENDAELE, M., WINDER, S., AND SZELISKI, R. 2003. High dynamic range video. *ACM Trans. Graph. 22*, 3, 319–325.

KHAN, E. A., REINHARD, E., FLEMING, R., AND BUELTHOFF, H. 2006. Image-based material editing. *ACM Transactions on Graphics (Proceedings of SIGGRAPH) 25*, 3 (July).

KRAWCZYK, G., MYSZKOWSKI, K., AND SEIDEL, H.-P. 2006. Computational model of lightness perception in high dynamic range imaging. In *Human Vision and Electronic Imaging XI, IS&T SPIE's 18th Annual Symposium on Electronic Imaging (2006)*, B. E. Rogowitz, T. N. Pappas, and S. J. Daly, Eds.

LANDIS, H. 2002. Production-ready global illumination. In *Siggraph Course Notes 16*.

LARSON, G. W., RUSHMEIER, H., AND PIATKO, C. 1997. A visibility matching tone reproduction operator for high dynamic range scenes. In *SIGGRAPH '97: ACM SIGGRAPH 97 Visual Proceedings: The art and interdisciplinary programs of SIGGRAPH '97*, ACM Press, New York, NY, USA, 155.

LEDDA, P., DOS SANTOS, L. P., AND CHALMERS, A. 2004. A local model of eye adaptation for high dynamic range. In *Proceedings of the 3rd International Conference on Computer Graphics, Virtual Reality, Visualisation and Interaction in Africa. AFRIGRAPH2004.*, ACM Press.

LEDDA, P., CHALMERS, A., TROSCIANKO, T., AND SEETZEN, H. 2005. Evaluation of tone mapping operators using a high dynamic range display. *ACM Trans. Graph. 24*, 3, 640–648.

LEVIN, A., LISCHINSKI, D., AND WEISS, Y. 2004. Colorization using optimization. *ACM Trans. Graph. 23*, 3, 689–694.

MANTIUK, R., MYSZKOWSKI, K., AND SEIDEL, H.-P. 2004. Visible difference predicator for high dynamic range images. In *Proceedings of IEEE International Conference on Systems, Man and Cybernetics*, 2763–2769.

MANTIUK, R., DALY, S., MYSZKOWSKI, K., AND SEIDEL, H.-P. 2005. Predicting visible differences in high dynamic range images - model and its calibration. In *Human Vision and Electronic Imaging X, IS&TSPIE's 17th Annual Symposium on Electronic Imaging*, B. E. Rogowitz, T. N. Pappas, and S. J. Daly, Eds., vol. 5666, 204–214.

PANOSCAN. http://www.panoscan.com/.

PATTANAIK, S., AND YEE, H. 2002. Adaptive gain control for high dynamic range image display. In *SCCG '02: Proceedings of*

the 18th spring conference on Computer graphics, ACM Press, New York, NY, USA, 83–87.

PATTANAIK, S. N., FERWERDA, J. A., FAIRCHILD, M. D., AND GREENBERG, D. P. 1998. A multiscale model of adaptation and spatial vision for realistic image display. In *SIGGRAPH '98: Proceedings of the 25th annual conference on Computer graphics and interactive techniques*, ACM Press, New York, NY, USA, 287–298.

PAVICIC, M. J. 1990. *Convenient Anti-Aliasing Filters that Minimize Bumpy Sampling*. Morgan Kaufmann.

PHARR, M., AND HUMPHREYS, G. 2004. *Improved infinite area light source sampling*. Morgan Kaufmann.

REINHARD, E., STARK, M., SHIRLEY, P., AND FERWERDA, J. 2002. Photographic tone reproduction for digital images. *ACM Trans. Graph. 21*, 3, 267–276.

REINHARD, E., WARD, G., PATTANAIK, S., AND DEBEVEC, P. 2005. *High Dynamic Range Imaging: Acquisition, Display and Image-Based Lighting*. Morgan Kaufmann Publishers, December.

REINHARD, E. 2002. Parameter estimation for photographic tone reproduction. *J. Graph. Tools 7*, 1, 45–52.

SEETZEN, H., HEIDRICH, W., STUERZLINGER, W., WARD, G., WHITEHEAD, L., TRENTACOSTE, M., GHOSH, A., AND VOROZCOVS, A. 2004. High dynamic range display systems. *ACM Trans. Graph. 23*, 3, 760–768.

SMITH, K., KRAWCZYK, G., MYSZKOWSKI, K., AND SEIDEL, H.-P. 2006. Beyond tone mapping: Enhanced depiction of tone mapped hdr images. *Computer Graphics Forum 25*, 3.

SPHERONVR. http://www.spheron.com/.

TUMBLIN, J., HODGINS, J. K., AND GUENTER, B. K. 1999. Two methods for display of high contrast images. *ACM Trans. Graph. 18*, 1, 56–94.

VDP-HDR. http://www.mpi-sb.mpg.de/resources/hdr/vdp/.

WARD, G., AND SIMMONS, M. 2005. Jpeg-hdr: A backwards-compatible, high dynamic range extension to jpeg. In *Proceedings of the Thirteenth Color Imaging Conference*.

WARD, G. 1994. A contrast-based scalefactor for luminance display. 415–421.

YEE, Y. H., AND PATTANAIK, S. N. 2003. Segmentation and adaptive assimilation for detail-preserving display of high-dynamic range images. *The Visual Computer 19*, 7-8, 457–466.
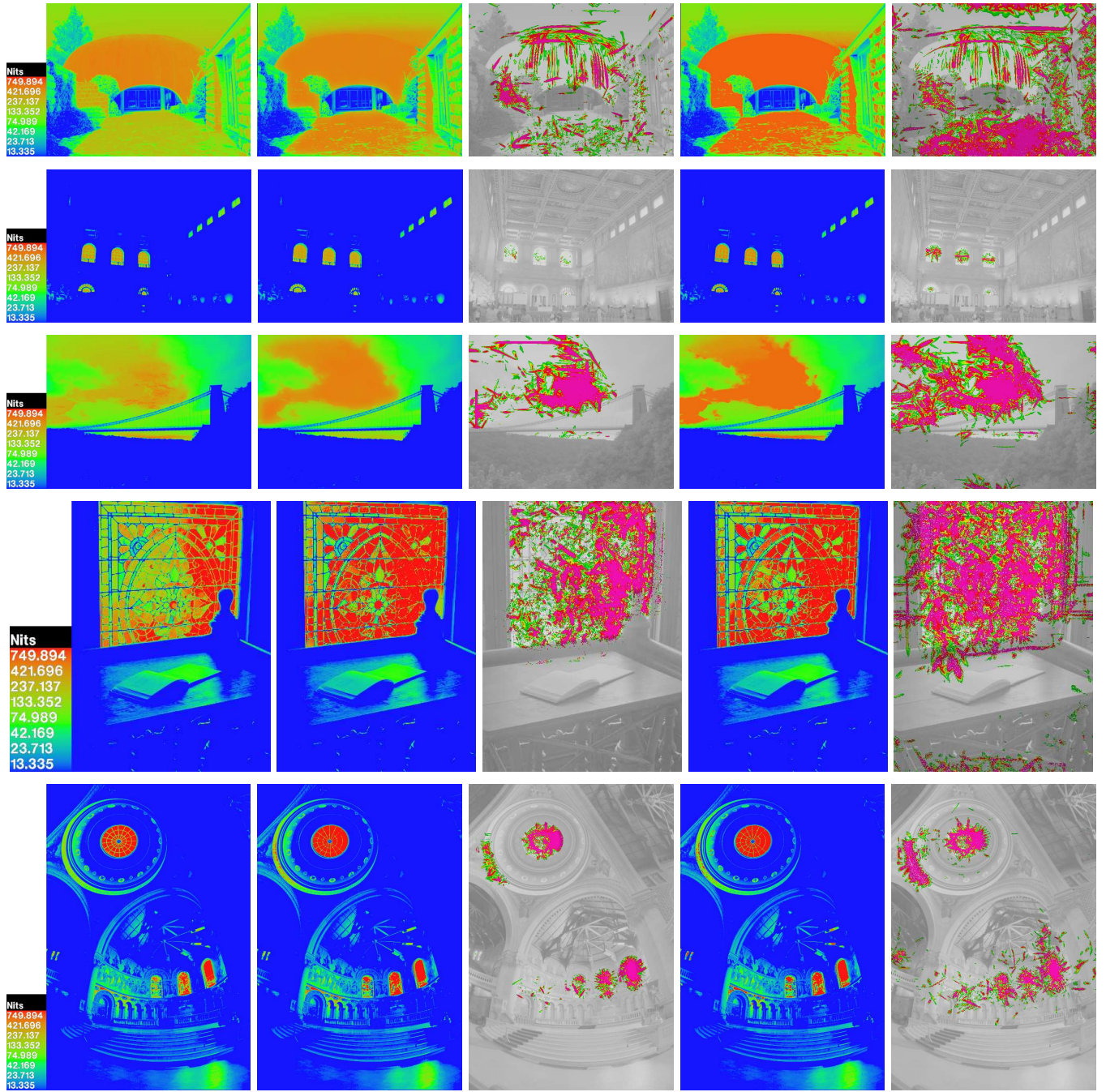
Figure 9: Examples of comparison for some images. For each row the first image is the radiance map of original HDRI, the second is the radiance map of the expanded LDRI using our algorithm. In the third is the VDP-HDR between the first and second image. Finally, the fourth image is the expanded LDRI using the *naive* algorithm and the fifth one is the result of VDP-HDR between the first and the fourth. The images comparisons shown are from top to bottom: Dani_Synagogue, ItalianMuseum1, BristolBridge, Desk_oBA2 image, and Memorial.